

Review

Review of External Humidifiers for Fuel Cells

Kai Li ¹, Wenxin Li ¹ and Jiang Liu ^{1,*}

¹ School of Mechanical and Automotive Engineering, Qingdao University of Technology, Qingdao, 266520, China

* Correspondence: Jiang Liu, School of Mechanical and Automotive Engineering, Qingdao University of Technology, Qingdao, 266520, China

Abstract: The efficient operation of Proton Exchange Membrane Fuel Cells (PEMFCs) relies on precise humidity control, and external humidification technology, which provides humidity management through independent devices, has become a key means to enhance system stability and durability. This article systematically reviews the latest advancements in external humidification technologies for PEMFCs, with a focus on membrane humidifiers, bubble humidifiers and spray humidifiers, analyzing their working principles, performance evaluation metrics and application scenarios. Research indicates that membrane humidifiers, with their low energy consumption and compact structure, hold an advantage in vehicular systems, but their performance is limited by membrane material lifespan and operational condition fluctuations. Bubble humidifiers demonstrate reliability in stationary applications, yet there is a pressing need for deeper research into their dynamic responses and mathematical modeling. Spray humidifiers achieve rapid humidification through direct water injection but are prone to "flooding" issues, necessitating optimization with high-precision control. The article also explores core evaluation metrics for humidifiers (such as dew point approach temperature, water vapor transfer rate, and pressure loss) and their impact on system performance, revealing the potential of novel structural designs like porous metal foams and biomimetic flow channels. Despite the significant improvements in humidity adaptability that external humidification technologies offer to PEMFCs, challenges such as increased system complexity, energy consumption control and long-term durability remain. Future research should focus on the collaborative optimization of various types of humidifiers, the development of intelligent control strategies and cross-disciplinary material innovations to promote their large-scale application in fields such as new energy vehicles and distributed energy systems.

Keywords: PEMFC; water management; external humidifier; humidification

Published: 27 March 2025



Copyright: © 2025 by the authors. Submitted for possible open access publication under the terms and conditions of the Creative Commons Attribution (CC BY) license (<https://creativecommons.org/licenses/by/4.0/>).

1. Introduction

Fuel cells, recognized for their efficiency and environmental benefits, have attracted considerable interest. These devices are capable of directly converting the chemical energy stored in fuel into electricity. By utilizing electrochemical reactions to convert the Gibbs free energy of fuel, fuel cells achieve remarkable efficiency in energy conversion. Fuel cells can be categorized according to their electrolyte composition and operational temperature. Low-temperature varieties include alkaline (AFC), phosphoric acid (PAFC), and proton exchange membrane (PEMFC) fuel cells, while high-temperature types consist of solid oxide (SOFC) and molten carbonate (MCFC) fuel cells [1]. Among them, PEMFCs stand out due to their advantageous features such as low-temperature operation, high energy density, rapid startup, robust load flexibility, broad application potential, and excellent efficiency [2,3]. As a result, PEMFCs are considered among the most promising technologies, with primary applications in distributed power generation, portable energy solutions and electric vehicles.

Figure 1 illustrates that the efficient operation of PEMFC relies on the integrated performance of several key systems, such as water management, thermal regulation, power generation, control, electrical, fuel supply and oxidant systems. A primary goal of the water management system is to optimize fuel cell efficiency and maintain stable long-term operation through effective water handling. Throughout the operation of a PEMFC, water is continually produced and exists in three states: vapor, liquid, and membrane-bound. The membrane-bound water, found in the electrolyte, is essential for keeping the membrane hydrated. Proper hydration is crucial as it ensures high proton conductivity, which is vital for peak fuel cell performance. However, when water accumulation becomes excessive, it can result in flooding [4], obstructing the gas diffusion layers and flow channels, thus impairing the transport of reactants to the reaction sites. This blockage reduces the catalyst's active area, leading to higher activation and concentration losses, and may even cause system shutdown. conversely, insufficient water levels lead to membrane dehydration, which increases electrical resistance and heat generation. This exacerbates drying and can result in membrane damage, significantly diminishing both performance and longevity [5]. Therefore, maintaining appropriate humidity is vital for optimal PEMFC operation.

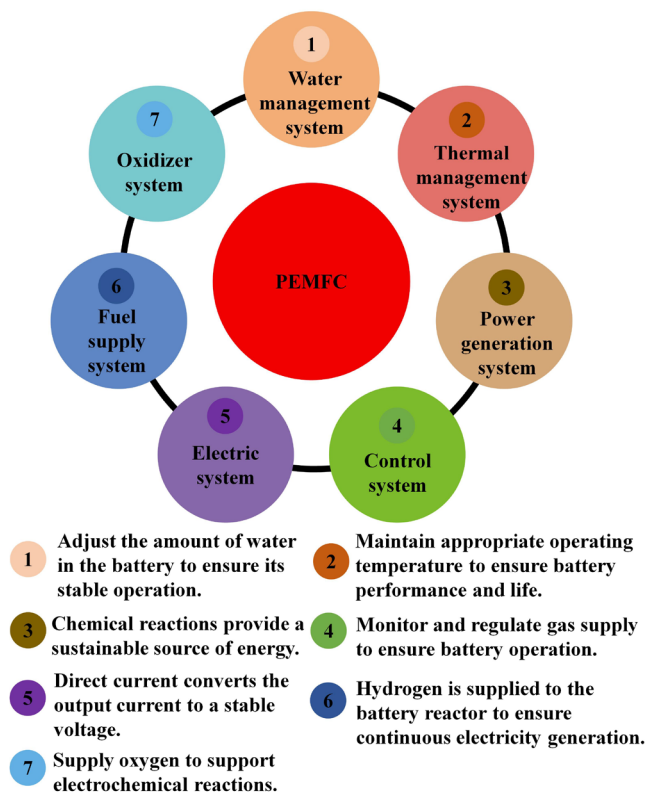


Figure 1. Composition of PEMFC system.

External humidification refers to the use of devices positioned outside the fuel cell to introduce moisture. Common techniques include membrane, bubble, spray, and sprinkler humidifiers. This article provides an overview of humidification methods for PEMFCs from the past five years, highlighting their underlying principles, benefits, limitations, and real-world applications. Additionally, it offers insights into effective humidity control strategies, supporting the optimization and advancement of fuel cells in various fields. By addressing key obstacles, this review seeks to direct future research toward innovation and progress.

2. Overall Performance Metrics for Humidifiers

In research on different humidifier types, performance evaluation criteria are established to explore the factors affecting humidifier efficiency and the impact of various operational parameters. Although these metrics are interrelated, they work together to offer a thorough evaluation of the humidifier's overall performance.

1) The dew point approach temperature

The Dew Point Approach Temperature quantifies the alignment between the humidity of the air exiting the humidifier and that of the incoming air. It represents the difference in dew point temperatures between the humidified air entering and the dry air leaving. Lowering the DPAT improves efficiency, and its optimal value is zero. The calculation of DPAT follows the equation (1) below.

$$\text{DPAT} = T_{wi} - T_{do} \quad (1)$$

Here, T_{wi} represents the dew point temperature of the humidified inlet air, while T_{do} represents the dew point of the dry exhaust air.

2) Water vapor flux

The Water Vapor Flux (WVF) quantifies the amount of water vapor passing through the membrane, shifting from the wet side to the dry side. Equation (2) illustrates this transfer process.

$$\text{WVTR} = \dot{m}_{v, \text{dry, out}} - \dot{m}_{v, \text{dry, in}} \quad (2)$$

Here, $\dot{m}_{v, \text{dry, out}}$ and $\dot{m}_{v, \text{dry, in}}$ represent the water vapor mass flow rates at the outlet and inlet of the dry side, respectively. These flow rates are determined through experimental measurements, including factors like relative humidity (RH) and temperature. For instance, the value of $\dot{m}_{v, \text{dry, out}}$ can be computed with the equation (3).

$$\dot{m}_{v, \text{dry, out}} = \omega_{\text{dry, out}} \dot{m}_{a, \text{dry}} \quad (3)$$

In this context, $\dot{m}_{a, \text{dry}}$ denotes the airflow rate on the dry side, while $\omega_{\text{dry, out}}$ represents the humidity ratio, which is determined using equation (4) below. In this formula, PPP refers to the system's operational pressure, whereas P_v corresponds to the partial pressure of water vapor.

$$\omega_{\text{dry, out}} = \frac{0.622P_v}{P - P_v} \quad (4)$$

3) Water transport rate

The water transport rate quantifies how efficiently water vapor moves across the exchange membrane, expressed as the ratio of the water vapor transmission rate to the membrane's total surface area. This metric serves as a key parameter for evaluating water mass transfer per unit area. The WVTR is determined by calculating the difference between the water mass flow rates at the dry side's outlet and inlet. The intensity of water transport depends on the driving forces acting across the membrane – greater forces, such as steeper moisture concentration gradients or elevated temperature differentials, lead to a higher transfer rate. Equation (5) describing water transport is provided below.

$$J = \frac{\text{WVTR}}{N \times A_m} = \frac{\dot{m}_{H_2O, do} - \dot{m}_{H_2O, di}}{N \times A_m} = \frac{(a_{do} - a_{di})Q}{N \times A_m} \quad (5)$$

In the equation, N represents the number of water exchange membranes, A_m is the effective water exchange area of a single water exchange membrane in the humidifier (m^2), $\dot{m}_{H_2O, do}$ is the mass flow rate of water in the dry outlet air stream (g/s), $\dot{m}_{H_2O, di}$ is the mass flow rate of water in the dry inlet air stream, a_{do} is the absolute humidity on the dry outlet air side (g/m^3), a_{di} is the absolute humidity on the dry inlet air side, and Q is the volumetric flow rate of dry air (m^3/s).

Within this equation, NNN denotes the total count of water exchange membranes, while A_m specifies the effective exchange surface area of an individual membrane inside the humidifier (m^2). The term $\dot{m}_{H_2O, do}$ refers to the mass flow rate of water in the outgoing dry air stream (g/s), whereas $\dot{m}_{H_2O, di}$ represents the corresponding mass flow rate at the inlet. Additionally, $\dot{m}_{H_2O, di}$ indicate the absolute humidity levels at the dry air outlet and inlet, respectively, measured in g/m^3 . Lastly, QQQ defines the volumetric flow rate of dry air (m^3/s).

4) Water recovery efficiency

The Water Recovery Rate serves as a key dimensionless parameter for evaluating water recycling effectiveness. A higher WRR indicates improved efficiency in transferring moisture from the humid air stream to the dry air flow. This metric is mathematically defined as the proportion of the Water Vapor Transfer Rate (WVTR) relative to the total water mass flow rate in the humid air stream [6]. The corresponding equation (6) is presented as follows.

$$\text{WRR} = \frac{\text{WVTR}}{\dot{m}_{\text{H}_2\text{O},wi}} = \frac{\dot{m}_{\text{H}_2\text{O},do} - \dot{m}_{\text{H}_2\text{O},di}}{\dot{m}_{\text{H}_2\text{O},wi}} = \frac{a_{do} - a_{di}}{a_{wi}} \times 100\% \quad (6)$$

Where $\dot{m}_{\text{H}_2\text{O},wi}$ is the water mass flow rate in the humid inlet air stream, and a_{wi} is the absolute humidity on the humid inlet air side.

In this equation, $\dot{m}_{\text{H}_2\text{O},wi}$ represents the mass flow rate of water within the incoming humid air stream, while a_{wi} denotes the absolute humidity on the inlet side of the humid air flow.

5) DS export dew point

The dew point refers to the temperature at which a gas reaches saturation with water vapor. The effectiveness of a humidifier improves when its DS outlet conditions closely match the optimal requirements of the fuel cell. As a result, higher humidity and temperature at the DS outlet signify better humidification performance. To assess this performance, the Dew Point Approach Temperature (DPAT) is introduced as a key indicator [7]. Ideally, the dew point at the DS outlet should be elevated to closely align with the dew point at the WS inlet.

6) Pressure loss

Pressure drop in the humidifier primarily results from two factors: (1) frictional energy dissipation caused by the interaction between dry and humid air within the flow channels, and (2) obstruction due to accumulated condensed water on the wet air side, which influences the pressure balance at the humidifier's inlet and outlet. This pressure reduction directly affects the power needed to circulate air, as greater losses necessitate increased energy input for air delivery into both the humidifier and the fuel cell. Consequently, optimizing channel dimensions to minimize pressure drop is a crucial consideration in humidifier design. The total pressure drop across the humidifier corresponds to the overall pressure differential between the dry and wet side flow channels, as defined by equation (7).

$$\Delta P = (P_{do} - P_{di}) + (P_{wo} - P_{wi}) \quad (7)$$

The pressures at the dry and wet sides' inlets and outlets are represented by P_{do} , P_{di} , P_{wo} and P_{wi} , respectively.

7) Performance efficiency ratio

Additionally, the effectiveness of a humidifier can be assessed using the Coefficient of Performance (COP) [8, 9]. COP quantifies the enthalpy change of dry air over time relative to the power consumed for air extraction. Equation (8) for COP is given as follows.

$$\text{COP} = \frac{(h_{do} - h_{di}) \times \dot{m}}{\Omega} \quad (8)$$

Here, \dot{m} denotes the mass flow rate of dry air, while h_{do} and h_{di} correspond to the specific enthalpy of dry air at the outlet and inlet, respectively. The term Ω represents the power dissipation resulting from pressure drop within the flow channels, which is determined using equation (9).

$$\Omega = Q \times \Delta P \quad (9)$$

Here, Q represents the volumetric airflow rate of dry air (m^3/s), while ΔP denotes the overall pressure drop (Pa) resulting from airflow resistance within the humidifier's dry and wet channels.

3. The Membrane Humidifier

Among the various types of humidifiers, membrane humidifiers stand out due to their low noise levels, simple structure, and ease of assembly. As a result, they have garnered more attention compared to other humidifiers. In a membrane humidifier, moist hot air (or liquid water) and dry air flow through channels on either side of the membrane. Driven by differences in concentration and temperature, water and heat are transferred through the membrane to the dry side, facilitating the humidification process. In contemporary automotive fuel cell systems, the moist, heated air from the cathode exhaust is commonly utilized to both warm and humidify the dry air entering the fuel cell stack. This establishes a close relationship between the membrane humidifier and the operating conditions of the fuel cell. Moreover, membrane humidifiers are essential in achieving a compact and optimized design for PEMFC systems [10]. Membrane humidifiers are classified into two main types based on their structure: flat membrane humidifiers and shell-and-tube humidifiers. This article begins by outlining the evaluation criteria for membrane humidifiers, followed by an in-depth analysis of each type.

3.1. Flat Membrane Humidifier

Flat membrane humidifiers are mainly considered as gas-to-gas devices. Investigations into these humidifiers typically examine the principles of heat and mass transfer, the effects of various operational factors, and how the design structure impacts performance. This paper synthesizes research on flat membrane humidifiers, highlighting both computational simulations and practical experiments.

3.1.1. Numerical Simulation of Membrane Humidifiers

Numerical simulations primarily reveal the underlying mechanisms of membrane humidifiers, including the simultaneous interactive effects of physical structure and operational parameters on humidifier performance. These insights provide guidance for determining design parameters and control strategies for humidifiers.

Initially, research on the factors influencing membrane humidifiers includes a study by T. Cahalan et al. who performed humidification experiments on various types of membranes [11]. They applied a lumped-parameter Fick's diffusion model, supplemented by a dimensionless function X , to assess membrane efficiency. By comparing the theoretical water vapor transfer rates of their model with experimental data, they concluded that sulfonated fluorinated membranes exhibited the highest vapor transfer capacity. Expanding on this, Ladislaus Schoenfeld et al. developed an analytical model that integrates mass and heat transfer, gas boundary layers [12], developing flow, and membrane characteristics under typical operating conditions. This model was verified using experimental results from pure Nafion® membranes as well as composite membranes. Their findings indicated that an increase in inlet relative humidity and Reynolds number enhanced permeation, while higher temperatures or pressures reduced it. The comparison between the model and the measured data for Nafion® 212 and 115 membranes demonstrated strong consistency. Additionally, they observed that the resistance of the boundary layer and membrane were similar in magnitude, and for channel Reynolds numbers below 2000, typical of automotive membrane humidifiers, the boundary layer resistance is significant and should not be overlooked.

Wei et al. conducted numerical simulations to study heat and mass transfer in membrane humidifiers with co-current and counter-current flow configurations [13]. They explored how factors like inlet temperature and mass flow rate in the wet and dry channels influenced pressure drop, dew point approach temperature, and water recovery rate. Their findings indicated that the dew point temperature increased with higher wet air inlet temperature and dry air mass flow rate, but decreased with a higher wet air mass flow rate and dry air inlet temperature. The water recovery rate was higher with elevated wet air inlet temperature and mass flow rate, with counter-current flow demonstrating

better humidification performance. In Figure 2a, Seyed Ze et al. used a numerical model to examine the effects of operational parameters [14], such as membrane properties, inlet temperatures, mass flow rates on both sides, and channel shapes (stepped, zigzag, and sinusoidal) on humidifier performance. They found that increasing the inlet temperature of both channels and the mass flow rate of water vapor improved humidification, in line with previous studies. Additionally, enhancing membrane porosity or permeability, lowering the gas channel mass flow rate, and reducing the thickness of the membrane's porous medium boosted humidifier efficiency. Among the tested channel geometries, the stepped structure yielded the best results. In their later study, they performed an in-depth numerical analysis on a cross-flow membrane humidifier with a 74-series module [15], investigating how variables like volumetric flow rate, dry air temperature, dew point wet temperature, and gas diffusion layer porosity influenced performance. They discovered that increasing volumetric flow rate raised water vapor transfer rates and dew point approach temperature, but decreased water recovery rate and relative humidity. Additionally, they observed that the pressure drops across the gas channels increased with flow rate, resulting in a higher power requirement for the humidifier.

N. Baharlou Houreh et al. were the first to investigate the effects of obstacle shape and quantity on membrane humidifier performance through numerical simulations [16]. As illustrated in Figure 2b, rectangular obstacles in humidifiers resulted in the highest water transfer rate, dew point at the dry-side outlet, and pressure drop. Additionally, it was found that using only one obstacle did not offer any benefits regarding pressure drop; at least two obstacles were required for improved humidification performance.

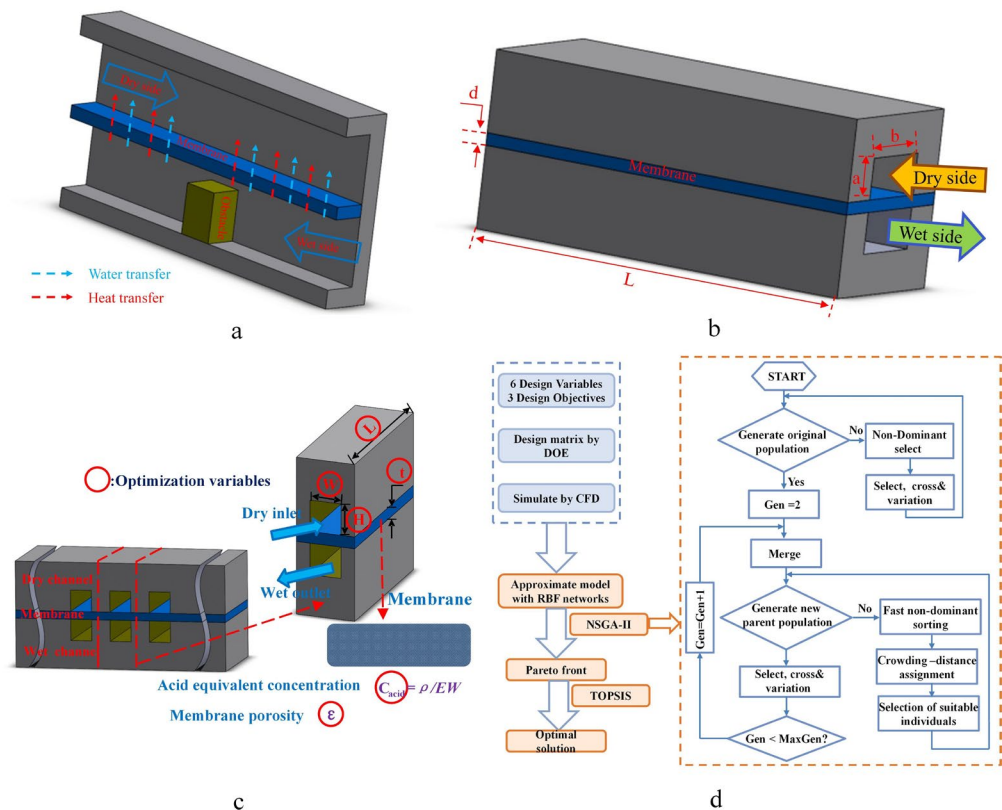


Figure 2. a. 3D schematic view of half the blocked membrane humidifier with single channel at dry and wet side, b. Schematic of the simple planar membrane humidifier considered, c. Membrane humidifier model and calculation domain d. The flow diagram of a multi-objective optimization and NSGA-II [16].

In later research [17], the authors introduced a thermal-hydraulic performance factor (JF) to assess the effectiveness of membrane humidifiers with partially blocked channels. The JF factor, defined in equation (10), reflects the balance between heat transfer efficiency and pressure drop, where higher values indicate superior performance. Their results showed that at low flow rates (below 4.4mg/s), blocked humidifiers performed less efficiently than simpler designs, even when pressure drop was not considered, suggesting that blockage should be avoided in such conditions. At medium flow rates (between 4.4mg/s and 6.65mg/s), blocked humidifiers were more efficient than simple ones, but when factoring in pressure drop, their overall performance was lower. At high flow rates (above 6.65mg/s), blocked humidifiers consistently outperformed simple humidifiers, regardless of pressure drop considerations.

$$JF = \frac{j}{f^{1/3}} \quad (10)$$

Here, j represents the Colburn factor for the wet-side flow channel, which indicates thermal performance (heat transfer) and f is the friction factor for the wet-side flow channel, representing hydraulic performance (pressure drop). The Colburn j factor describes the relationship between convective heat transfer, fluid properties, geometry, and operating conditions, as expressed below. In this equation, Nu and Re are the Prandtl number and Reynolds number, respectively

In this context, j represents the Colburn factor, which quantifies the thermal performance (heat transfer) in the wet-side flow channel, while f denotes the friction factor, reflecting hydraulic performance (pressure drop) in the same channel. The Colburn factor j links convective heat transfer, fluid properties, geometry, and operational conditions, as shown in equation (11) below. In this expression, Nu and Re represent the Nusselt number and Reynolds number, respectively.

$$j = \frac{Nu}{RePr^{1/3}} \quad (11)$$

Lu et al. performed numerical simulations to examine the influence of five different flow channel geometries — equilateral triangle [18], isosceles triangle, square, rectangle, and semicircle — on water transport efficiency and pressure drop. They identified three key geometric factors — centroid height, perimeter, and hydraulic diameter—to characterize these shapes. Their findings revealed a significant relationship between the water transport performance and the centroid height of the flow channel cross-section, with lower centroid heights improving humidification efficiency. Additionally, they observed that the Darcy-Weisbach equation, which includes the Poiseuille number to account for the cross-sectional geometry, offers more precise pressure loss predictions than the Hagen-Poiseuille equation. These insights provide valuable theoretical guidance for designing flat membrane humidifiers.

Recently, the powerful capabilities and rapid development of combining meta-models with optimization algorithms have garnered significant attention. These approaches are particularly well-suited for physical models involving the interactive effects of various operational parameters and physical structures and have been widely applied to multi-objective optimization problems in fuel cells [19-23]. As shown in Figures 2c and 2d, building on their previous work [18], Li et al. employed a radial basis function (RBF) neural network combined with a numerical simulation-based experimental design method. They specified channel height, width, and length, as well as membrane thickness, porosity, and acid concentration as design variables, with humidification capacity, pressure loss, and occupied volume as optimization objectives. This approach studied the impact of humidifier design parameters on performance and guided the determination of optimal design parameters [24]. The results showed that channel dimensions — length, width, and height — had the greatest effect on humidification efficiency and pressure drop, far exceeding the impact of membrane-related parameters. This approach effectively optimizes multiple objectives for flat membrane humidifiers, balancing performance, pressure loss, and space usage.

3.1.2. Experimental Studies

Experimental studies offer greater intuitiveness and reliability. Research on membrane humidifiers primarily focuses on the effects of operational parameters and physical structures through experimental investigations.

Florian Wolfenstetter et al. conducted experiments to explore how humidity [25], pressure, and temperature influenced membrane permeability. They tested three Nafion® membranes of varying thicknesses (211, 212, 115) as well as a composite membrane from W.L. Gore & Associates. The study found that humidity had the strongest effect on permeability, while absolute pressure mainly impacted diffusion in the adjacent gas boundary layers rather than within the membrane itself. Temperature increase raised the diffusion coefficients in both the boundary layer and the membrane, but reduced water adsorption in the polymer membrane. Thicker Nafion® membranes exhibited lower permeability at higher temperatures, while the Gore composite membrane's permeability remained unchanged with temperature fluctuations. As shown in Figure 3, membranes with thinner selective layers demonstrated higher overall permeability, with the Gore composite membrane achieving the highest permeability and Nafion® 115 the lowest. The findings also revealed that Nafion® 211, although thinner than Nafion® 212, did not have double the permeability, as the total resistance involves diffusion in both the gas boundary layer and the membrane itself. Thinner membranes had a larger proportion of boundary layer resistance, providing a theoretical foundation for their subsequent analytical model [12].

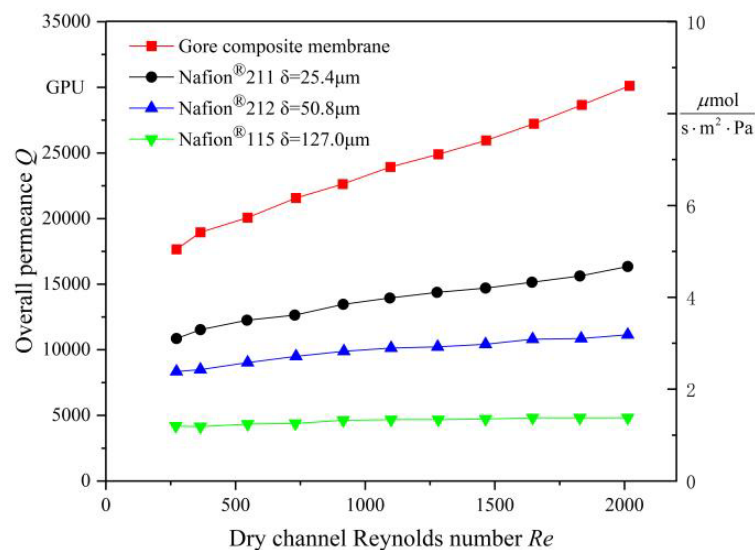


Figure 3. Overall permeance of Nafion® 211, 212, 115 and the experimental composite membrane by W. L. Gore & Associates at $T = 350\text{K}$, $\text{RH} = 90\%$ and $p = 2.5\text{bar}$ [25].

Chen et al. found that increasing the air flow rate boosts the water vapor transfer rate [26]. However, once the flow rate surpasses an optimal level, further increases do not lead to improvements in the dew point approach temperature or water recovery rate, despite a higher WVTR. Additionally, higher dry air inlet temperatures reduce the water vapor concentration gradient across the membrane, resulting in lower WVTR and WRR. In their subsequent study [9], they explored how channel dimensions and operating conditions affect humidification performance. The results showed that increasing channel depth improves performance by increasing the cross-sectional area. Among channels with equal cross-sectional areas, wider channels provided better humidification. Their findings also indicated that lower flow rates, dry air inlet temperatures, and relative humidity enhanced humidification efficiency.

The performance of humidifiers can be influenced by the flow configurations and the structure of the channels. N. Baharlou Houreh et al. were among the first to experimentally compare cross-flow [6], parallel-flow, and counter-flow configurations. Their results showed that counter-flow designs outperformed others, while parallel-flow configurations were the least efficient. Additionally, they noted that increasing the dry-side flow rate improved both the water recovery rate (WRR) and the dew point approach temperature (DPAT). Under different boundary conditions, they observed that with a dry-side inlet temperature of 30°C and a wet-side inlet temperature of 60°C, the WRR was higher than in 60°C isothermal conditions but lower than under 30°C isothermal conditions. They also found that the DPAT under adiabatic conditions was closer to the 60°C isothermal case, yet substantially higher than the 30°C isothermal one, highlighting the significance of the wet-side inlet temperature on humidifier performance. N. Masaeli et al. conducted a comparative analysis of humidifiers with serpentine, finned and simple parallel channels [27], focusing on mass transfer, heat transfer, and pressure loss. Figure 4 illustrates the performance evaluation metrics (PEC) for serpentine and finned channels. As indicated in Figure 4a, finned channels had a pressure drop comparable to parallel channels, while serpentine channels had a significantly higher pressure drop. Serpentine channels improved both heat and water transfer performance but resulted in higher pressure losses. Figure 4b reveals that the PEC for serpentine channels remained above 1 across various dry-side flow rates, indicating superior overall performance. As the flow rate increased from 0.4m³/h to 1m³/h, the PEC decreased from 2.58 to 1.47. Serpentine channels were more effective at lower flow rates, while finned channels performed better at higher flow rates due to their lower pressure drops, despite offering comparable PEC.

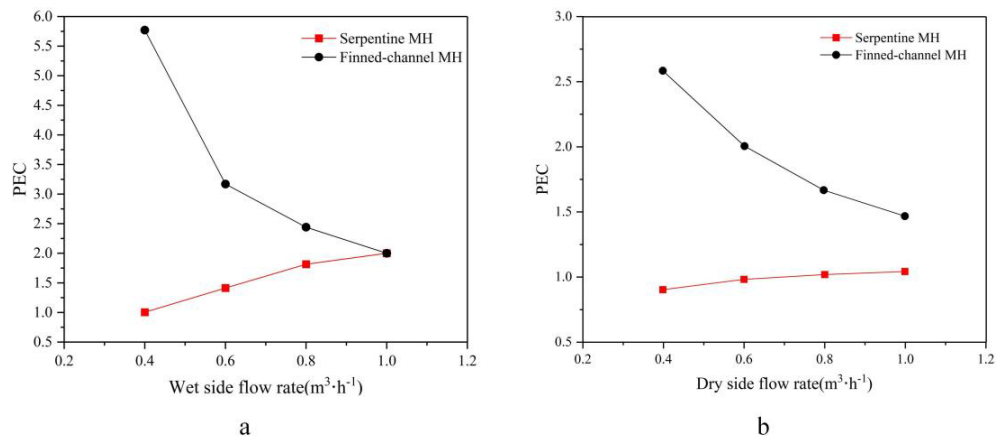


Figure 4. The humidifier PEC of serpentine channel and fin channel. a. Changes in PEC with respect to WS flow rate and b. Changes in PEC with respect to DS flow rate [27].

3.2. Shell-and-Tube Humidifiers

Shell-and-tube membrane humidifiers are mainly used for gas-to-liquid humidity transfer. Similar to flat membrane humidifiers, research in this field can be categorized into two primary areas: the development of mechanistic models and the investigation of physical configurations.

In mechanistic model research, Miguel Solsona et al. developed a model for a low-temperature PEMFC cathode humidifier that was validated experimentally [28]. This model, aimed at controlling and monitoring the humidification process, was derived from analyzing the mass and heat transfer dynamics of circulating air. They constructed a non-linear fourth-order multi-input/multi-output system model, which was verified through experimental results. Hoang Nghia Vu et al. explored the role of membrane humidifiers in regulating the humidity of cathode air [29]. They compared two configurations involving humidifier bypass with supply and exhaust flows to control the relative humidity of

the cathode inlet. Their study showed that using a humidifier bypass for the supply air helped maintain a stable cathode inlet humidity across a wide range of operating conditions. M. Schmitz et al. created a three-dimensional model of a tubular membrane humidifier using computational fluid dynamics (CFD) [30]. They developed an empirical model to describe how convection in the airflow promotes adsorption. Their CFD model incorporated empirical data through derived formulas, leading to accurate predictions of humidifier behavior. However, they found that temperature did not significantly enhance adsorption, and discrepancies appeared in their model when the wet air flow rate exceeded the dry air flow rate, indicating a need for further investigations. Despite these limitations, their research offers valuable insights for improving the accuracy of future humidifier models. In proton exchange membrane fuel cells, porous metal foams have gained considerable attention for their ability to enhance heat and mass transfer, owing to their high thermal conductivity [31-33]. However, their low electrical conductivity and the complexity of fuel cell stack structures limit their fabrication and application. In contrast, applying metal foams to humidifiers to enhance performance is more feasible, but related research is scarce. At the mechanistic level, previous studies created idealized models, but these theoretical models had limitations. Hyesoo Jang et al. built upon these efforts by developing fluid models for metal foam channels and heat transfer models for humidifiers [34]. They investigated how various types of porous metal foams in flow channels affect the heat and mass transfer characteristics of shell-and-tube membrane humidifiers. They also evaluated metal foam humidifiers under various operational conditions and configurations to determine the most effective combination for enhancing efficiency.

Xuan Linh Nguyen et al. examined membrane modules in humidifiers under isothermal conditions to assess how operational factors influence vapor diffusion [35]. Their study revealed that temperature and wet-side relative humidity played key roles in determining vapor transport rates. They also established new formulas to relate diffusion coefficients to temperature, humidity, and pressure, yielding an R-squared value close to 0.9. In a subsequent investigation [36], they integrated experimental and modeling approaches to evaluate the performance of hollow fiber membrane humidifiers. The membrane humidifier model is depicted in Figure 5a, with Figure 5b showcasing the vapor transport mechanism. Their analysis focused on how parameters such as temperature, flow rate, pressure, and humidity affect water transport in the system. Using response surface methodology, they established regression models for four key operating parameters, demonstrating the impact of these factors and their interactions on humidifier performance. Sensitivity studies revealed that temperature, relative humidity, and flow rate were positively correlated with performance, while pressure was negatively correlated.

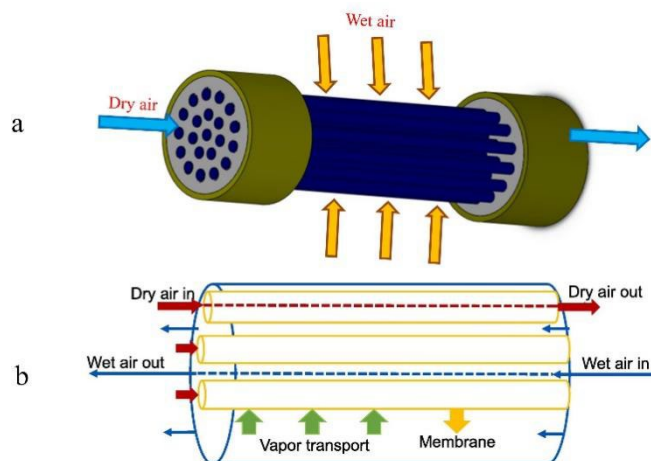


Figure 5. a. A tubular membrane module and b. Mechanism of vapor transport through the membrane [36].

4. Bubble Humidification

Bubble humidifiers and spray humidifiers are structurally simple and reliable, offering superior humidification performance. They are primarily used in various fixed systems such as testing systems, large ferries, and power generation systems.

Bubble humidification is a commonly used external humidification method for PEMFC systems. Bubble humidifiers operate by directing reaction gases through high-temperature deionized water, where they form bubbles, facilitating humidification through heat and mass transfer. Though commonly applied in stationary fuel cell systems, there is still limited research on their performance. A major area of investigation has been the effects of different parameters on their output characteristics. Rajalakshmi et al. explored how the size and number of holes in the gas distributor influence bubble humidifier performance [37]. Their findings showed that as the distributor's diameter increases, relative humidity also rises, particularly when the diameter is scaled from micrometers to millimeters. However, the impact of the hole count on performance is not straightforward; it varies depending on the deionized water's temperature and the gas flow rate. Ahmaditaba et al., as shown in Figure 6a [38], studied the effects of water temperature, liquid level, and gas flow rate on the performance of bubble humidifiers. Their research indicated that increasing the temperature and water level in the deionized water enhanced humidification, while a higher gas flow rate resulted in reduced humidification efficiency.

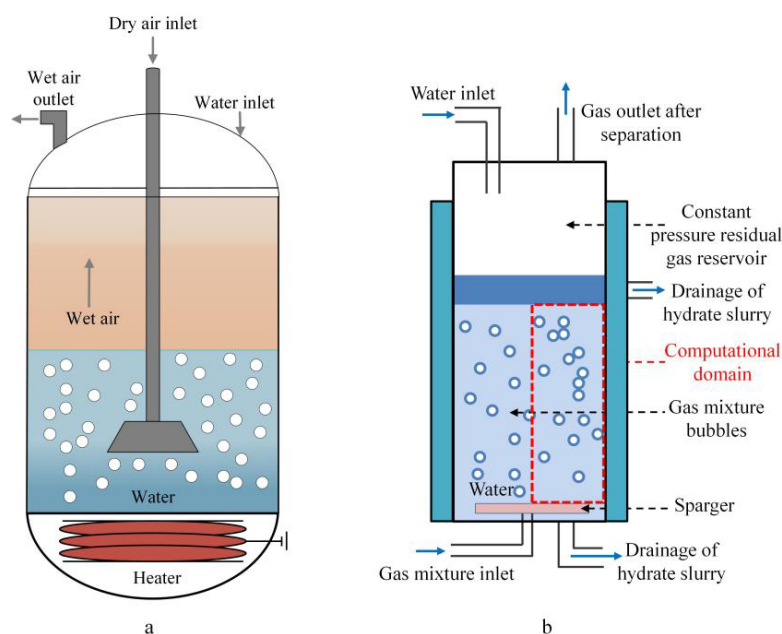


Figure 6. a. Schematic of bubble humidifier and b. bubble column reactor schematic for continuous hydrate formation.

Although bubble humidifiers have garnered interest, much of the existing research focuses on experimental studies, with relatively few investigations into their mathematical modeling. Theoretical studies on bubble humidifiers can be divided into three key aspects: gas-liquid phase fluid dynamics, mass transfer, and heat transfer. The operational principles and designs of bubble humidifiers closely resemble those of bubble column reactors, which are commonly used in processes like seawater desalination and evaporation crystallization. Since the fluid dynamics of bubble column reactors have been extensively researched, bubble humidifiers can benefit from these insights and apply similar analyses to study their fluid dynamics in the context of desalination processes [39-41]. For instance, Tsuchiya et al. examined the impact of pressure and temperature on bubble size and flow

velocity in bubble columns [42], establishing a foundation for understanding bubble behavior and flow dynamics in humidifier systems [43, 44]. However, these models and theoretical calculations cannot provide detailed flow field information inside the column. CFD (Computational Fluid Dynamics) offers more detailed, visual and comprehensive information than theoretical models and has been widely applied to gas-liquid two-phase simulations.

Xiaoyun Guo used a CFD-PBM (Population Balance Model) coupled method to study liquid flow and bubble evolution and interactions in a jet bubble column [45], validating the model's accuracy through experiments. The Population Balance Model is commonly employed to study phenomena such as gas holdup, bubble distribution, and the processes of bubble coalescence and breakup in bubble columns. However, selecting the right sub-models for these columns can be quite challenging. To address this complexity, Zhang et al. explored the use of the class method (CM) in CFD-PBM simulations of bubble columns and introduced an optimization approach for determining the values of critical parameters [46]. The CM consists of four parameters: the volume ratio between continuous bubble classes (rv), the minimum diameter (d_{min}), the maximum diameter and the critical diameter (d_c) used to differentiate between small and large bubbles. Their study focused on examining the impact of these parameters through numerical simulations of two representative bubble columns and comparing the simulation results with experimental data.

In the realm of gas-liquid mass and heat transfer, Aritra Kar et al. created a detailed mechanistic model that addresses the mass transfer, heat transfer and various interfacial phenomena associated with gas hydrate formation in bubble column reactors [47], as illustrated in Figure 6b. This model facilitates the analysis of how operational factors such as gas flow rate, bubble size, reactor pressure, inlet gas temperature, and reactor geometry influence the rates of hydrate formation and the conversion efficiency of gas to hydrate. To enhance the performance of mass and heat transfer, bubble columns are frequently outfitted with fillers like glass beads and corrugated plates. Huang et al. proposed an advanced gas-liquid heat and mass transfer model for humidifiers, incorporating both bubble and filler elements, which proved to accurately predict the internal dynamics of humidifiers. Their findings highlighted that the most effective way to boost humidifier performance was by increasing the liquid inlet temperature. Additionally, they observed that in these systems, the air temperature and humidity levels increased in a wave-like fashion along the column's height, with the primary driving forces for heat and mass transfer being the temperature and humidity differences at both ends of the humidifier.

Bubble humidifiers are capable of delivering adequate humidification for an extended period, even during power outages, without the need for external energy input [48]. This feature makes them particularly ideal for use in power plants and testing systems.

5. Spray Humidification

Spray humidification involves injecting water directly into the fuel cell inlet in liquid or vapor form using external components such as atomizers or spray humidifiers, also known as the direct water injection method. Since spray humidification using atomizers is primarily applied in mobile systems and represents a true direct water injection method, while spray humidifiers share a similar large-volume tank structure with bubble humidifiers, this article will discuss atomizer-based humidification and spray humidification separately.

5.1. Atomizer-Based Humidification

Sung et al. utilized ultrasonic atomizing nozzles for humidification [49]. These nozzles can produce smaller water droplets by adjusting the driving frequency, thereby

providing higher humidification efficiency. Yasuda et al. investigated the actual atomization volume in ultrasonic atomization [50]. Ultrasonic atomization involves both atomization and liquid evaporation, and the evaporation volume can be estimated by simulating ultrasonic spray using pumps and nozzles, which helps determine the actual atomization volume. This is particularly useful in scenarios requiring precise control of atomization volume. Meanwhile, this ultrasonic atomization method has been widely applied in methanol fuel cell feeding systems [51-55]. Li et al. experimentally compared the performance differences between liquid feeding and ultrasonic atomization feeding, finding a 31.8% improvement in cell performance. This technique works effectively for atomized air intake and cooling systems, particularly under high current densities with large volumes of reaction gases and heat. However, the use of spray humidification can lead to excessive water being introduced into the fuel cell, potentially causing "flooding" [56, 57]. Zhang et al. proposed a new air humidifier design combining heat exchange and spray humidification for a 5kW fuel cell system operating at elevated temperatures [58]. To prevent flooding, they employed a precise flow meter to control the liquid water flow rate. Nevertheless, the flooding issue continues to hinder the progress of spray-based humidification. Additionally, pumping losses and high energy consumption remain significant challenges for this design.

5.2. Spray Humidification

Spray humidification systems typically consist of a spray chamber, spray nozzles, and a demister [58]. Dry air enters the spray chamber from the bottom and mixes with droplets sprayed from the nozzles at the top to achieve humidification. Verhage et al. presented an experimental 70kW PEM power plant that integrated a spray tower humidifier within its system. In a similar context [59], Hao Hu et al. developed a three-dimensional CFD model for a swirling spray humidifier, performing numerical simulations to examine the coupled heat and mass transfer within the humidifier [60]. The simulation results, shown in Figure 7, highlight the dynamic load characteristics. In the swirling spray humidifier setup, dry air enters tangentially from the base and is mixed with droplets from centrally positioned nozzles. Their analysis revealed that the best humidification performance occurred with a single nozzle and a spray temperature set to 300K. The team also explored the outlet humidity variations under different load conditions.

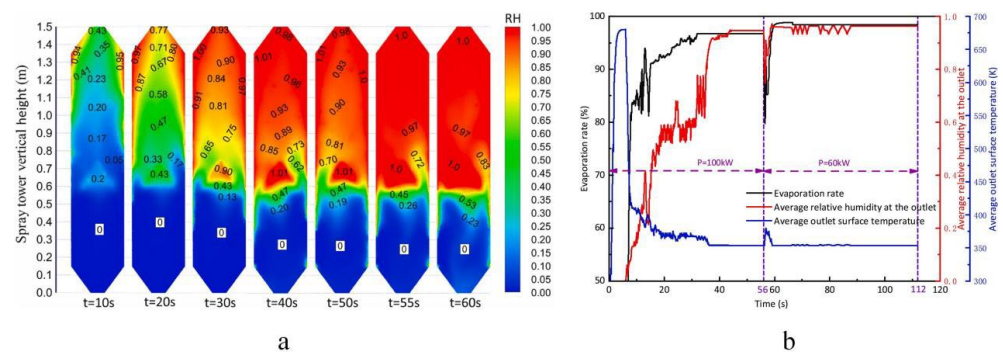


Figure 7. a. Variation of relative humidity over time and b. High-power humidifier load characteristics.[60].

Beyond basic nozzle spray humidifier designs, spray humidifiers can also be integrated with other types such as packed-bed or bubble humidifiers. For example, Ma et al. developed a spray humidifier with nozzles positioned at the tank's top [61], while maintaining water inside the tank for bubble-based humidification. Initially, the gas undergoes humidification via bubbles, then interacts with the spray from the nozzles at the top to enhance both mass and heat transfer, leading to improved humidification efficiency. This

type of humidification system is straightforward, dependable, and highly effective, making it widely used in stationary humidification systems. While spray humidifiers have been extensively studied in solar desalination of seawater [62-66], comprehensive research into their use for PEM fuel cell humidification is still quite limited.

This spray humidification technique stands out for its straightforward design and high versatility, which makes it commonly employed in stationary humidification systems, including those used in power generation and testing apparatus. For instance, companies like Canada's GREENLIGHT, Japan's HORIBA, Austria's AVL, and China's Kewell have adopted this spray humidification approach.

6. Conclusion

This article explores external humidification techniques for Proton Exchange Membrane Fuel Cells (PEMFC), which utilize humidification devices within the external loop to hydrate the membrane. It mainly covers membrane, bubble, and spray humidifiers. External humidifiers are characterized by their simple structure, excellent humidification performance, and reliability. However, due to the increased system complexity, they are typically used in fixed installations such as testing systems and power generation systems. Among the different methods, membrane humidifiers are particularly notable for having no moving components and not requiring an external power source, making them highly suitable for portable applications. As a result, they have received considerable attention in research. However, their performance is greatly dependent on the operating conditions, and issues related to the membrane's lifespan and durability remain significant challenges. These areas are crucial for further investigation and enhancement. Additionally, controlling the humidification process with precision is complex and needs further refinement within the system framework. While bubble and spray humidifiers are in widespread use, research on them is still limited, and their practical application demands careful design considerations. Studies on structural optimization are scarce, and there is a need to explore dynamic response issues in more detail. Overall, each humidification method has its own set of pros and cons. In various practical settings, it is important to evaluate factors such as system complexity, weight, volume, and efficiency to guarantee the success of the humidification system. Future studies should prioritize the development of materials and structures for both fuel cells and humidifiers, optimizing system designs, and advancing modeling techniques to propel the progress and implementation of humidification technologies.

References

1. M. Haslinger and T. Lauer, "Unsteady 3D-CFD simulation of a large active area PEM fuel cell under automotive operation conditions—efficient parameterization and simulation using numerically reduced models," *Processes*, vol. 10, no. 8, p. 1605, 2022, doi: 10.3390/pr10081605.
2. Q. Hassan, I. D. J. Azzawi, A. Z. Sameen, and H. M. Salman, "Hydrogen fuel cell vehicles: opportunities and challenges," *Sustainability*, vol. 15, no. 15, p. 11501, 2023, doi: 10.3390/su151511501.
3. X. Lü, Y. Qu, Y. Wang, C. Qin, and G. Liu, "A comprehensive review on hybrid power system for PEMFC-HEV: issues and strategies," *Energy Convers. Manag.*, vol. 171, pp. 1273–1291, 2018, doi: 10.1016/j.enconman.2018.06.065.
4. Z. Bao, Z. Niu, and K. Jiao, "Gas distribution and droplet removal of metal foam flow field for proton exchange membrane fuel cells," *Appl. Energy*, vol. 280, p. 116011, 2020, doi: 10.1016/j.apenergy.2020.116011.
5. G. Zhang and K. Jiao, "Multi-phase models for water and thermal management of proton exchange membrane fuel cell: a review," *J. Power Sources*, vol. 391, pp. 120–133, 2018, doi: 10.1016/j.jpowsour.2018.04.071.
6. N. Baharlou Houreh, M. Ghaedamini, H. Shokouhmand, E. Afshari, and A. H. Ahmadi, "Experimental study on performance of membrane humidifiers with different configurations and operating conditions for PEM fuel cells," *Int. J. Hydrogen Energy*, vol. 45, no. 7, pp. 4841–4859, 2020, doi: 10.1016/j.ijhydene.2019.12.017.
7. S. Yu, S. Im, S. Kim, J. Hwang, Y. Lee, S. Kang, and K. Ahn, "A parametric study of the performance of a planar membrane humidifier with a heat and mass exchanger model for design optimization," *Int. J. Heat Mass Transf.*, vol. 54, no. 7, pp. 1344–1351, Mar. 2011, doi: 10.1016/j.ijheatmasstransfer.2010.11.054.

8. C.-Y. Chen, Y.-H. Chang, C.-H. Li, C.-C. Chang, and W.-M. Yan, "Physical properties measurement and performance comparison of membranes for planar membrane humidifiers," *Int. J. Heat Mass Transf.*, vol. 136, pp. 393–403, 2019, doi: 10.1016/j.ijheatmasstransfer.2019.03.027.
9. W.-M. Yan, C.-Y. Chen, Y.-k. Jhang, Y.-H. Chang, P. Amani, and M. Amani, "Performance evaluation of a multi-stage plate-type membrane humidifier for proton exchange membrane fuel cell," *Energy Convers. Manag.*, vol. 176, pp. 123–130, 2018, doi: 10.1016/j.enconman.2018.09.027.
10. H. Pourrahmani, M. Moghimi, M. Siavashi, and M. Shirbani, "Sensitivity analysis and performance evaluation of the PEMFC using wave-like porous ribs," *Appl. Therm. Eng.*, vol. 150, pp. 433–444, 2019, doi: 10.1016/j.applthermaleng.2019.01.010.
11. T. Cahalan, S. Rehfeltd, M. Bauer, M. Becker, and H. Klein, "Analysis of membranes used in external membrane humidification of PEM fuel cells," *Int. J. Hydrogen Energy*, vol. 42, no. 22, pp. 15370–15384, 2017, doi: 10.1016/j.ijhydene.2017.03.215.
12. L. Schoenfeld, M. Kreitmair, F. Wolfenstetter, M. Neumann, H. Klein, and S. Rehfeltd, "Modeling mass and heat transfer in membrane humidifiers for polymer electrolyte membrane fuel cells," *Int. J. Heat Mass Transf.*, vol. 223, 2024, doi: 10.1016/j.ijheatmasstransfer.2024.125260.
13. W.-M. Yan, C.-Y. Lee, C.-H. Li, W.-K. Li, and S. Rashidi, "Study on heat and mass transfer of a planar membrane humidifier for PEM fuel cell," *Int. J. Heat Mass Transf.*, vol. 152, 2020, doi: 10.1016/j.ijheatmasstransfer.2020.119538.
14. S. Z. Hashemi-Valikboni, S. S. M. Ajarostaghi, M. A. Delavar, and K. Sedighi, "Numerical prediction of humidification process in planar porous membrane humidifier of a PEM fuel cell system to evaluate the effects of operating and geometrical parameters," *J. Therm. Anal. Calorim.*, vol. 141, no. 5, pp. 1687–1701, 2020, doi: 10.1007/s10973-020-10058-6.
15. S. A. Atyabi, E. Afshari, and M. Y. Abdollahzadeh Jamalabadi, "Three-dimensional multiphase flow modeling of membrane humidifier for PEM fuel cell application," *Int. J. Numer. Methods Heat Fluid Flow*, vol. 30, no. 1, pp. 54–74, 2019, doi: 10.1108/HFF-03-2019-0263.
16. N. B. Houreh, H. Shokouhmand, and E. Afshari, "Effect of inserting obstacles in flow field on a membrane humidifier performance for PEMFC application: A CFD model," *Int. J. Hydrogen Energy*, vol. 44, no. 57, pp. 30420–30439, 2019, doi: 10.1016/j.ijhydene.2019.09.189.
17. N. B. Houreh, E. Afshari, H. Shokouhmand, and S. Asghari, "Numerical study and experimental validation on heat and water transfer through polymer membrane by applying a novel enhancement technique," *J. Energy Storage*, vol. 29, p. 101387, 2020, doi: 10.1016/j.est.2020.101387.
18. C. Lu, Y. Li, Z. Liu, H. Zhou, H. Zheng, and B. Chen, "Influence mechanisms of flow channel geometry on water transfer and pressure loss in planar membrane humidifiers for PEM fuel cells," *Int. J. Hydrogen Energy*, vol. 47, no. 91, pp. 38757–38773, 2022, doi: 10.1016/j.ijhydene.2022.09.049.
19. Y. Amadane and H. Mounir, "Performance improvement of a PEMFC with dead-end anode by using CFD-Taguchi approach," *J. Electroanal. Chem.*, vol. 904, p. 115909, Jan. 2022, doi: 10.1016/j.jelechem.2021.115909.
20. Z. Chen, W. Zuo, K. Zhou, Q. Li, Y. Huang, and J. E, "Multi-factor impact mechanism on the performance of high temperature proton exchange membrane fuel cell," *Energy*, vol. 278, p. 127982, Sep. 2023, doi: 10.1016/j.energy.2023.127982.
21. Y. Li, Z. Ma, M. Zheng, D. Li, Z. Lu, and B. Xu, "Performance analysis and optimization of a high-temperature PEMFC vehicle based on particle swarm optimization algorithm," *Membranes*, vol. 11, no. 9, p. 691, 2021, doi: 10.3390/membranes11090691.
22. S. M. Pourkiaei, F. Pourfayaz, M. Mehrpooya, and M. H. Ahmadi, "Multi-objective optimization of tubular solid oxide fuel cells fed by natural gas: An energetic and exergetic simultaneous optimization," *J. Therm. Anal. Calorim.*, vol. 145, no. 3, pp. 1575–1583, 2021, doi: 10.1007/s10973-021-10849-5.
23. H. Edwards, M. P. Pereira, S. Gharaie, R. Omrani, and B. Shabani, "Computational fluid dynamics modelling of proton exchange membrane fuel cells: Accuracy and time efficiency," *Int. J. Hydrogen Energy*, vol. 50, pp. 682–710, 2024, doi: 10.1016/j.ijhydene.2023.09.004.
24. Y. Li, H. Chen, C. Lu, H. Zhou, Z. Liu, and B. Chen, "Multi-objective optimization design of a planar membrane humidifier based on NSGA-II and entropy weight TOPSIS," *J. Therm. Anal. Calorim.*, vol. 148, no. 14, pp. 7147–7161, 2023, doi: 10.1007/s10973-023-12202-4.
25. F. Wolfenstetter, M. Kreitmair, L. Schoenfeld, H. Klein, M. Becker, and S. Rehfeltd, "Experimental study on water transport in membrane humidifiers for polymer electrolyte membrane fuel cells," *Int. J. Hydrogen Energy*, vol. 47, no. 55, pp. 23381–23392, 2022, doi: 10.1016/j.ijhydene.2022.05.114.
26. C.-Y. Chen, W.-M. Yan, C.-N. Lai, and J.-H. Su, "Heat and mass transfer of a planar membrane humidifier for proton exchange membrane fuel cell," *Int. J. Heat Mass Transf.*, vol. 109, pp. 601–608, 2017, doi: 10.1016/j.ijheatmasstransfer.2017.02.045.
27. N. Masaeli, E. Afshari, E. Baniasadi, N. Baharlou-Houreh, and M. Ghaedamini, "Experimental analysis of water transfer and thermal-hydraulic performance of membrane humidifiers with three flow field designs," *Appl. Energy*, vol. 336, p. 120823, 2023, doi: 10.1016/j.apenergy.2023.120823.
28. M. Solsona, C. Kunusch, and C. Ocampo-Martinez, "Control-oriented model of a membrane humidifier for fuel cell applications," *Energy Convers. Manag.*, vol. 137, pp. 121–129, 2017, doi: 10.1016/j.enconman.2017.01.036.
29. H. N. Vu, D. H. Trinh, D. T. L. Tri, and S. Yu, "Bypass configurations of membrane humidifiers for water management in PEM fuel cells," *Energies*, vol. 16, no. 19, p. 6986, 2023, doi: 10.3390/en16196986.

30. M. Schmitz, F. Welker, S. Tinz, M. Bahr, S. Gössling, S. Kaimer, and S. Pischinger, "Comprehensive investigation of membrane sorption and CFD modeling of a tube membrane humidifier with experimental validation," *Int. J. Hydrogen Energy*, vol. 48, no. 23, pp. 8596–8612, 2023, doi: 10.1016/j.ijhydene.2022.11.081.
31. G. Zhang, Z. Bao, B. Xie, Y. Wang, and K. Jiao, "Three-dimensional multi-phase simulation of PEM fuel cell considering the full morphology of metal foam flow field," *Int. J. Hydrogen Energy*, vol. 46, no. 3, pp. 2978–2989, 2021, doi: 10.1016/j.ijhydene.2020.05.263.
32. D. G. Kang, D. K. Lee, J. M. Choi, D. K. Shin, and M. S. Kim, "Study on the metal foam flow field with porosity gradient in the polymer electrolyte membrane fuel cell," *Renew. Energy*, vol. 156, pp. 931–941, 2020, doi: 10.1016/j.renene.2020.04.142.
33. E. Afshari, "Computational analysis of heat transfer in a PEM fuel cell with metal foam as a flow field," *J. Therm. Anal. Calorim.*, vol. 139, no. 4, pp. 2423–2434, 2020, doi: 10.1007/s10973-019-08354-x.
34. H. Jang, M. H. Kim, S. K. Park, Y. S. Kim, and B. C. Choi, "Simulation of heat and mass transfer characteristics for the optimal operating conditions of a gas-to-gas membrane humidifier with porous metal foam," *Energies*, vol. 13, no. 19, p. 5110, 2020., doi: 10.3390/en13195110.
35. X. L. Nguyen, H. N. Vu, and S. Yu, "Parametric understanding of vapor transport of hollow fiber membranes for design of a membrane humidifier," *Renew. Energy*, vol. 177, pp. 1293–1307, 2021, doi: 10.1016/j.renene.2021.06.003.
36. V. K. Phan, X. L. Nguyen, Y. Choi, D. T. L. Tri, H. L. Nguyen, and S. Yu, "Water transport analysis of hollow fiber membrane humidifier module using response surface method," *Therm. Sci. Eng. Prog.*, vol. 49, 2024, doi: 10.1016/j.tsep.2024.102453.
37. N. Rajalakshmi, P. Sridhar, and K. S. Dhathathreyan, "Identification and characterization of parameters for external humidification used in polymer electrolyte membrane fuel cells," *J. Power Sources*, vol. 109, no. 2, pp. 452–457, Jul. 2002, doi: 10.1016/S0378-7753(02)00102-7.
38. A. H. Ahmaditaba, E. Afshari, and S. Asghari, "An experimental study on the bubble humidification method of polymer electrolyte membrane fuel cells," *Energy Sources, Part A: Recovery, Utilization, Environ. Eff.*, vol. 40, no. 12, pp. 1508–1519, 2018, doi: 10.1080/15567036.2018.1477877.
39. J. Chen et al., "Characteristic analysis of heat and mass transfer process within structured packing humidifier," *J. Braz. Soc. Mech. Sci. Eng.*, vol. 41, no. 9, 2019, doi: 10.1007/s40430-019-1864-y.
40. P. R. R. Raj and J. S. Jayakumar, "Performance analysis of humidifier packing for humidification dehumidification desalination system," *Therm. Sci. Eng. Prog.*, vol. 27, p. 101118, 2022, doi: 10.1016/j.tsep.2021.101118.
41. X. Huang, H. Chen, X. Ling, L. Liu, and T. Huhe, "Investigation of heat and mass transfer and gas–liquid thermodynamic process paths in a humidifier," *Energy*, vol. 261, p. 125156, 2022, doi: 10.1016/j.energy.2022.125156.
42. T. J. Lin, K. Tsuchiya, and L. S. Fan, "Bubble flow characteristics in bubble columns at elevated pressure and temperature," *AIChE J.*, vol. 44, no. 3, pp. 545–560, 1998, doi: 10.1002/aic.690440306.
43. N. Çarşıbaşı, F. Borak, and K. Ulgen, "Bubble column reactors," *Process Biochem.*, vol. 40, pp. 2263–2283, Aug. 2005, doi: 10.1016/j.procbio.2004.10.004.
44. H. A. Jakobsen, H. Lindborg, and C. A. Dorao, "Modeling of bubble column reactors: Progress and limitations," *Ind. Eng. Chem. Res.*, vol. 44, no. 14, pp. 5107–5151, Jul. 2005, doi: 10.1021/ie049447x.
45. X. Guo et al., "Evolution and interaction characteristics of liquid flow and bubbles in a jet bubbling column," *Ind. Eng. Chem. Res.*, vol. 59, no. 48, pp. 21217–21230, Dec. 2020, doi: 10.1021/acs.iecr.0c04178.
46. X.-B. Zhang, R.-Q. Zheng, and Z.-H. Luo, "CFD-PBM simulation of bubble columns: Effect of parameters in the class method for solving PBEs," *Chem. Eng. Sci.*, vol. 226, p. 115853, 2020., doi: 10.1016/j.ces.2020.115853.
47. A. Kar and V. Bahadur, "Analysis of coupled heat & mass transfer during gas hydrate formation in bubble column reactors," *Chem. Eng. J.*, vol. 452, p. 139322, 2023, doi: 10.1016/j.cej.2022.139322.
48. G. Vasu, A. K. Tangirala, B. Viswanathan, and K. S. Dhathathreyan, "Continuous bubble humidification and control of relative humidity of H₂ for a PEMFC system," *Int. J. Hydrogen Energy*, vol. 33, no. 17, pp. 4640–4648, 2008, doi: 10.1016/j.ijhydene.2008.05.051.
49. C.-C. Sung, C.-Y. Bai, J.-H. Chen, and S.-J. Chang, "Controllable fuel cell humidification by ultrasonic atomization," *J. Power Sources*, vol. 239, pp. 151–156, Oct. 2013, doi: 10.1016/j.jpowsour.2013.03.076.
50. K. Yasuda, H. Honma, Z. Xu, Y. Asakura, and S. Koda, "Ultrasonic atomization amount for different frequencies," *Jpn. J. Appl. Phys.*, vol. 50, no. 7S, 2011, doi: 10.1143/JJAP.50.07HE23.
51. T. Li, Z. Ye, S. Gong, C. Wu, and W. Zhan, "Studies on the temperature characteristics of an ultrasonic atomization feed direct methanol fuel cell," in *Proc. Int. Conf. Mech. Design*, Singapore: Springer Nature Singapore, Aug. 2021, pp. 811–827. ISBN: 9789811673818.
52. C. Wu, S. Gong, S. Hu, and Z. Ye, "Experimental studies on the performances of a direct methanol fuel cell with a novel integrated ultrasonic atomization fuel feeder," *Fuel Cells*, vol. 20, no. 2, pp. 158–165, 2020, doi: 10.1002/face.201900147.
53. R. K. Mallick, S. B. Thombre, and N. K. Shrivastava, "Vapor feed direct methanol fuel cells (DMFCs): A review," *Renew. Sustainable Energy Rev.*, vol. 56, pp. 51–74, 2016, doi: 10.1016/j.rser.2015.11.039.
54. W. Yuan, B. Zhou, J. Deng, Y. Tang, Z. Zhang, and Z. Li, "Overview on the developments of vapor-feed direct methanol fuel cells," *Int. J. Hydrogen Energy*, vol. 39, no. 12, pp. 6689–6704, 2014, doi: 10.1016/j.ijhydene.2014.02.002.

55. H.-N et al., "Numerical simulation on mass transport in a passive vapor-fed direct methanol fuel cell operating with neat methanol," *J. Power Sources*, vol. 477, p. 228541, 2020, doi: 10.1016/j.jpowsour.2020.228541.
56. P. Moçotéguy, B. Ludwig, D. Beretta, and T. Pedersen, "Study of the impact of water management on the performance of PEMFC commercial stacks by impedance spectroscopy," *Int. J. Hydrogen Energy*, vol. 45, no. 33, pp. 16724–16737, 2020, doi: 10.1016/j.ijhydene.2020.04.139.
57. O. S. Ijaodola et al., "Energy efficiency improvements by investigating the water flooding management on proton exchange membrane fuel cell (PEMFC)," *Energy*, vol. 179, pp. 246–267, 2019, doi: 10.1016/j.energy.2019.04.074.
58. S. H. Jung, S. L. Kim, M. S. Kim, Y. Park, and T. W. Lim, "Experimental study of gas humidification with injectors for automotive PEM fuel cell systems," *J. Power Sources*, vol. 170, no. 2, pp. 324–333, Jul. 2007, doi:10.1016/j.jpowsour.2007.04.013.
59. A. J. L. Verhage, J. F. Coolegem, M. J. J. Mulder, M. H. Yildirim, and F. A. de Bruijn, "30,000 h operation of a 70kW stationary PEM fuel cell system using hydrogen from a chlorine factory," *Int. J. Hydrogen Energy*, vol. 38, no. 11, pp. 4714–4724, Apr. 2013, doi: 10.1016/j.ijhydene.2013.01.152.
60. H. Hu et al., "CFD investigation of a fast-response humidifier for high-power PEMFC test stations," *Int. J. Hydrogen Energy*, vol. 52, pp. 1056–1069, 2024, doi: 10.1016/j.ijhydene.2023.06.301.
61. T. Ma et al., "Numerical study on humidification performance of fuel cell test platform humidifier," *Energies*, vol. 12, no. 20, p. 3839, 2019, doi: 10.3390/en12203839.
62. J. Yu, S. Jin, and Y. Xia, "Experimental and CFD investigation of the counter-flow spray concentration tower in solar energy air evaporating separation saline wastewater treatment system," *Int. J. Heat Mass Transfer*, vol. 144, p. 118621, Dec. 2019, doi: 10.1016/j.ijheatmasstransfer.2019.118621.
63. K. Srithar and T. Rajaseenivasan, "Recent fresh water augmentation techniques in solar still and HDH desalination—A review," *Renewable Sustainable Energy Rev.*, vol. 82, pp. 629–644, Feb. 2018, doi: 10.1016/j.rser.2017.09.056.
64. R. Dhivagar and S. Sundararaj, "A review on methods of productivity improvement in solar desalination," *Appl. Mech. Mater.*, vol. 877, pp. 414–429, 2018, doi: 10.4028/www.scientific.net/AMM.877.414.
65. B. Zhang, Y. Niu, and P. Guo, "Establishment of reaction engineering approach for saline droplet and its application in spray evaporation simulation," *Desalination*, vol. 575, p. 117330, 2024, doi: 10.1016/j.desal.2024.117330.
66. Ma, X., Shi, W., and Yang, H., "Spray parameter analysis and performance optimization of indirect evaporative cooler considering surface wettability," *J. Build. Eng.*, vol. 82, p. 108175, 2024, doi: 10.1016/j.jobbe.2023.108175.

Disclaimer/Publisher's Note: The statements, opinions and data contained in all publications are solely those of the individual author(s) and contributor(s) and not of SOAP and/or the editor(s). SOAP and/or the editor(s) disclaim responsibility for any injury to people or property resulting from any ideas, methods, instructions or products referred to in the content.